Journal of
Marine Science and Engineering

MDPI

Article

Potential Hydrodynamic Impacts and Performances of Commercial-Scale Turbine Arrays in the Strait of Larantuka, Indonesia

Kadir Orhan * and Roberto Mayerle

Research and Technology Centre Westcoast (FTZ), University of Kiel, 24118 Kiel, Germany; rmayerle@corelab.uni-kiel.de

* Correspondence: kadir.orhan@yandex.com; Tel.: +49-179-654-0886

Received: 12 February 2020; Accepted: 19 March 2020; Published: 22 March 2020

Abstract: The Strait of Larantuka, with highly energetic tidal stream currents reaching speeds of up to 3–4 m/s, is a promising site for renewable electricity production from the ocean. This paper presents the results of an assessment regarding the potential hydrodynamic impacts, wake characteristics, and the performances of large scale turbine arrays in the strait. A high-resolution, three-dimensional baroclinic model is developed using the FLOW module of the Delft3D modeling system to simulate tidal currents. The energy of currents is assumed to be extracted by horizontal-axis tidal turbines, which can harness strong bi-directional flow, positioned on sequential rows and alternating downstream arrangements. Enhanced momentum sinks are used to represent the influence of energy extraction by the tidal turbines. Four different array layouts with rated capacities of up to 35 MW are considered. We find that, in the Strait of Larantuka, array layout significantly affects the flow conditions and the power output, mainly due to the geometric blockage effect of the bounded channel. With respect to undisturbed flow conditions in the strait, decreases in current speeds of up to about 0.6 m/s, alongside increases in the order of 80% near-shore are observed. While operating efficiency rates of turbines reaching around 50%–60% resulted during the spring tide in the arrays with smaller rated capacities, the power output of the devices was negligible during the neap tide.

Keywords: tidal stream current; tidal energy extraction; numerical model; Indonesia

1. Introduction

Intergovernmental Panel on Climate Change (IPCC) recently reported on the current and potential impacts of anthropogenic global warming. The report states that human activities have caused a warming of 1.0 °C above the pre-industrial levels since 1950, with a rate of increase of 0.2 °C per decade, and global warming is likely to reach 1.5 °C between 2030 and 2052. Storms, forest fires, droughts, coral bleaching, heat waves, and floods, which have already been experienced due to global warming, are likely to get significantly worse in the upcoming decades, and impacts are expected to be felt across ecosystems, human communities, and economies [1]. The mitigation of further damage requires an effective and appropriate response focused on accelerating the reduction of global greenhouse gas emissions. Thus, over the last few decades, ocean renewable energy (ORE) has become a promising alternative and supplement to fossil fuels and nuclear power. ORE might enhance the diversity of the energy mix, contribute to the decarbonization of electricity production, increase energy security by exploiting local resources, and fuel economic growth in the coastal regions. To this end, the conversion of tidal current power is recently growing up to a crucial sector of the ORE [2,3]. Tidal electricity, with high quality and high predictability, can become an essential part of the high-penetration renewable energy electricity grids in the future [4].

The Strait of Larantuka, located in the eastern part of the Indonesian archipelago, divides East Flores from Adunara Island (see Figure 1). The strait is circa (ca.) 3 km in length. Around the bottleneck, which is the area of interest for this study, the channel width is ca. 650 m, and the water depth along the mid-channel is around 30–35 m. The Strait of Larantuka links the Flores Sea in the north to the Flores Strait in the south. While the predicted tidal amplitude in the Flores Sea is slightly larger than 1 m, it reaches around 1.5 m in the Flores Strait. Alongside the large quantities of tidal power input from the adjoining Indian and Pacific oceans [5], the straits between the Indian Ocean and inner Indonesian seas, such as the Strait of Larantuka, are under the influence of Indonesian throughflow (ITF). The exchange of water and heat from the Pacific Ocean to the Indian Ocean occurs through ITF [6–8], which is capable of modulating tidal stream resources within these domains [9]. Tidal currents in Indonesian straits could also show significant changes due to the density gradients and wind-induced circulation [10].

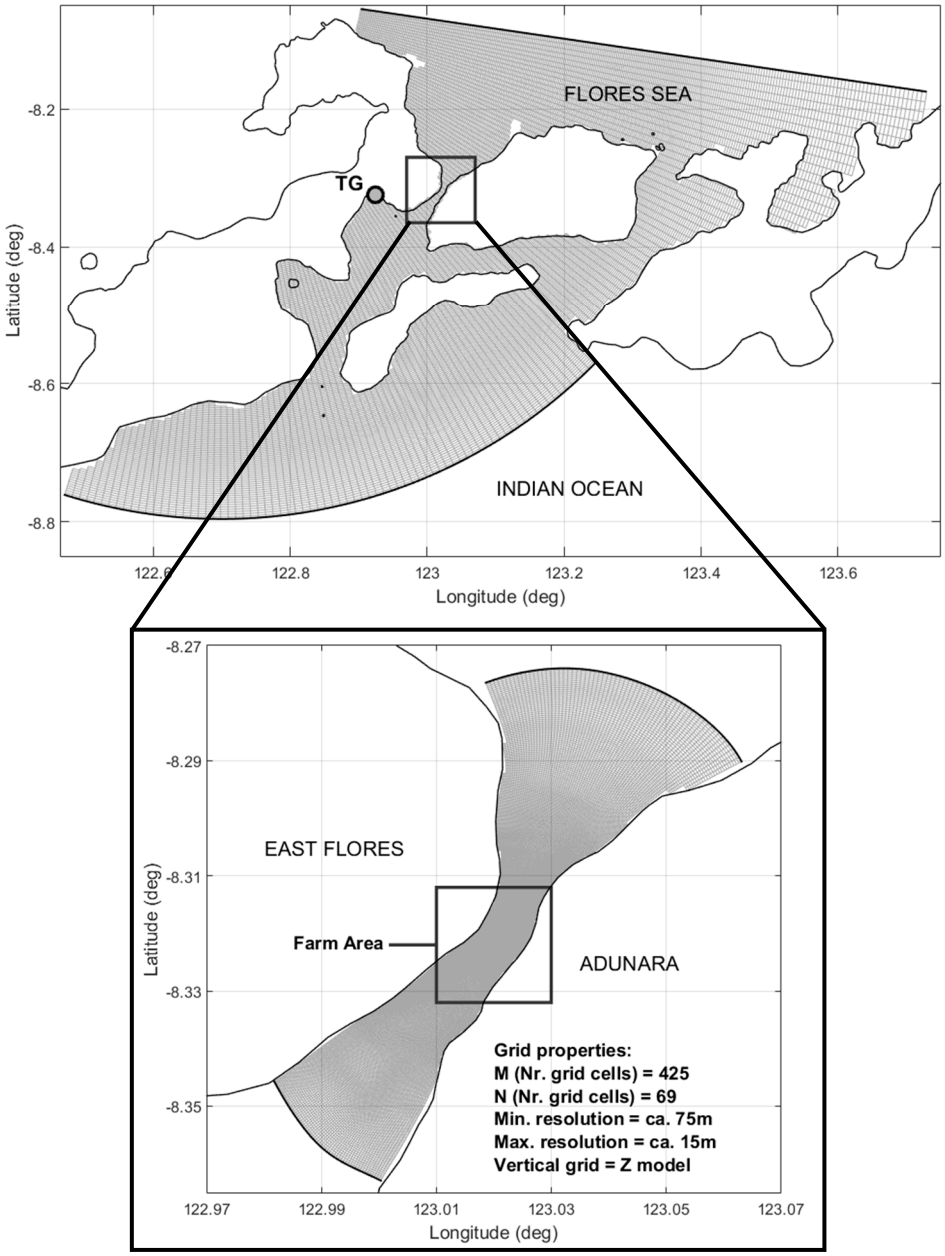

Figure 1. Nesting sequence of the computational grids for the Strait of Larantuka.

Previously, tidal stream resources of several promising straits between the Indian Ocean and inner Indonesian seas, including the Strait of Larantuka, have been investigated [11,12]. Orhan et al. (2017) provided an overview regarding the energy potential of tidal stream currents within the straits in question, utilizing state-of-the-art measurements and high-resolution, three-dimensional (3D) flow models. The results of this study showed that the highly energetic tidal stream currents of the Strait of Larantuka have tremendous potential for renewable electricity production. Current speeds in the strait exceed 3 m/s during peak periods while the kinetic power densities reach ca. 10 kW/m^2. Hence the Strait of Larantuka was proven suitable for the deployment of second generation tidal stream technologies, which are assumed to be capable of exploiting currents with peak spring flows above 2 m/s [13]. Another detailed analysis concerning the tidal stream resources of the strait, utilizing state-of-the-art modeling tools and field measurements, has been provided by Ajiwibowo et al. (2017) [14]. Ajiwibowo et al. (2017) agree with the results provided by Orhan et al. (2017) and provide a more detailed understanding of the renewable electricity generation potential in the strait. Therefore, the strait is of commercial interest [15], and the energy hotspot of the strait, encompassing an area around 3 km^2, provides enough space for ORE development. In a follow-up study, Orhan and Mayerle (2017) studied the possible impacts of the tidal turbines on flow conditions in the Strait of Larantuka. For this purpose, the computational grid of the hydrodynamic model used by Orhan et al. (2017) was refined, and a practical method to study the far-field impacts of the devices for different dissipation levels was adopted. Thus, the turbine wakes, wake recoveries, and velocity deficits in the adjacent areas due to the tidal current energy extraction were resolved in more detail. Firdaus et al. (2019) also examined interaction between the turbine arrays and the flow in the Strait of Larantuka and estimated average power available at several array locations [15,16].

This study, as an extension of the earlier studies mentioned above, aims at exploring the influence of turbine array capacity and layout on flow conditions, power output of the turbine arrays, and individual turbine performances. In the Strait of Larantuka, where increasing array sizes might cause significant alterations on the flow field due to the geometric blockage effect, this information might prove essential for future planning and development efforts. To this end, as previously done by Orhan and Mayerle (2017), high resolution, three-dimensional hydrodynamic models representing the tidal energy extraction, by introducing a momentum sink term into the momentum equations in the horizontal direction, are used for the investigations. Turbine arrays with various capacities and layouts are studied to investigate the changes in the flow field, wake characteristics, and array performances. Finally, efficiencies of tidal turbines are evaluated for the proposed layouts through a simplistic approach.

2. Methodology and Application

Tidal stream currents were computed with the FLOW module of the Delft3D Modeling System, developed by Deltares, the Netherlands [17,18]. Bathymetric data for the hydrodynamic models have been obtained from single beam echo sounding surveys and SRTM15_PLUS land and sea topography global dataset [19,20]. An overall model to simulate flow conditions in several interlinked straits, including the Strait of Larantuka, was developed with horizontal grid spacing around 300 m (Figure 1, top). Open boundaries of the overall model were extended into the Flores Sea in the north, and the Indian Ocean in the south to capture the input from both systems. To simulate the flow conditions in the Strait of Larantuka with greater resolution, a detailed model of the strait was nested into the overall model (Figure 1, bottom). The computational grid of the detailed model was constructed with a resolution up to ca. 16 m in horizontal and 2–3 m in vertical within the area of interest (i.e., farm area), providing sufficient spatial resolution for the analysis of hydrodynamic impacts from isolated tidal turbines. By this way, the tidal energy extraction was parameterized in 3D as an enhanced momentum sink to accurately evaluate the impacts and performances of individual turbines [21,22]. Z-layers fixed in the vertical direction were preferred in models for the accuracy of the vertical distribution of salinity and temperature [23].

In view of the potential influence of the wind-induced circulation and resulting density gradients [10], as well as the interaction between the Indonesian throughflow and the tidal currents [9], the tide-only approach was thought to be inadequate for the target domain. Therefore, much attention has been given to the meteorological forcing and conditions at the open sea boundaries to adequately capture the density gradients and flow fields along the strait. Tidal forcing is extracted from TOPEX/Poseidon Global Inverse Solution tidal model (TPXO) Indian Ocean Atlas (1/12° regional model) and prescribed as time series [24]. Eleven harmonic constituents (M2, S2, N2, K2, K1, O1, P1, Q1, M4, MS4, and MN4) were taken into account. Data to determine the salinity and the temperature at the open sea boundaries are supplied from Hamburg Shelf Ocean Model (HAMSOM), which is a 3D free surface baroclinic hydrodynamic model [7]. Data from the Global Forecast System of the National Oceanic and Atmospheric Administration (NOAA) National Climatic Data Center have been used as meteorological input [25]. Thus, the effects of air cloudiness, air temperature, atmospheric pressure, relative air humidity, and wind (in East (E) and North (N) directions) have been considered in simulations. To account for the exchange of heat through the free surface, the ocean heat flux module of Delft3D is activated, which typically applies to large water bodies [26]. Bottom roughness is computed according to the Chézy formula, and a uniform friction coefficient of 65 $m^{1/2}/s$ was defined throughout the model domain [18]. K-epsilon (k-ε) model is selected to include more adequately the effects of the turbulent kinetic energy and turbulent kinetic energy dissipation in simulations [27,28].

Time steps of 3s and 1s were set for the overall model and the detailed model, respectively. The chosen time steps correspond to a maximum Courant–Friedrichs–Lewis criterion of around 0.5 for both models. Earlier studies concerning the Strait of Larantuka [11,12,14,15] present the tidal current energy potential of the strait through the simulations covering a monthly period. This study mainly aims at analyzing the changes occurring in the flow field with increasing turbine array capacities, as well as wake characteristics and performances of tidal turbines. Therefore, although results concerning the entire neap-spring tidal cycle as well as individual neap and spring tidal cycles are provided, the emphasis was given to the conditions during a peak spring tide. This period, with particularly high current speeds, was chosen to analyze the flow field, turbine wake characteristics, and turbine array performances while the current speeds are sufficient for devices to operate and provide electric output.

The ability of the overall model to simulate water level elevations has been verified through tide gauge measurements. Figure 1, top panel, indicates the location of the measuring device. Figure 2 displays the comparison of simulated and measured tidal water levels for July 2014. The agreement between modeled and measured values was checked with Pearson's product-moment correlation coefficient (r) and root-mean-square deviation (RMSD). RMSD and r values resulted respectively equal to 0.11 m and 0.99, indicating a strong, positive linear relationship.

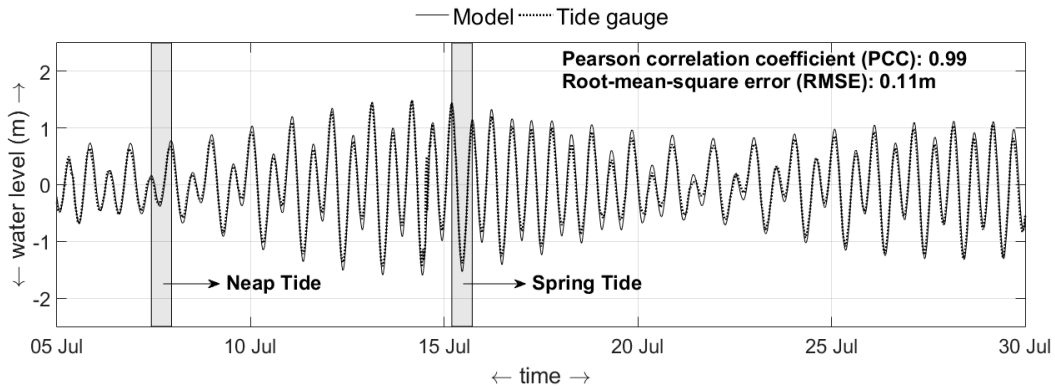

Figure 2. Comparison of modeled and measured tidal water levels at the tide gauge (TG) location (see Figure 1) during July 2014. Grey bars indicate the neap and spring tidal cycles considered for the analysis.

The energy of the tidal currents in the strait is assumed to be extracted by horizontal-axis tidal turbines, positioned on sequential rows, and in alternating downstream arrangements where the flow is bounded by the seabed and the free surface. Tidal turbines, much like wind turbines, are capable of extracting energy from a moving fluid. They feature blades with airfoil cross-sections and operate due to the principles of aerodynamic lift [29]. The design turbine in this study has been described based on the properties of actual, commercially available tidal turbines [3,29]. The device, which can harness a strongly bi-directional flow, was assumed to have a rotor diameter of ca. 16 m corresponding to a swept area of ca. 201 m^2. The minimum operational depth of the device was considered as 25 m. Rated, cut-in, and cut-out current speeds of the device were defined as 3.0 m/s, 1.0 m/s, and 4.5 m/s, respectively, and its rated power is ca. 1 MW. Considering the efficiencies of the various components, namely the turbine rotor, drive train, generator, and grid connection, the turbine power coefficient has been assumed as 0.41 [11,12,29]. The spacing between rows and lateral spacing between the devices was set to about 10 RD (rotor diameter) and 3 RD, respectively [12,30,31]. Figure 3 shows the arrangement of the turbines over the computational grid and bathymetric conditions within the proposed farm area (see Figure 1).

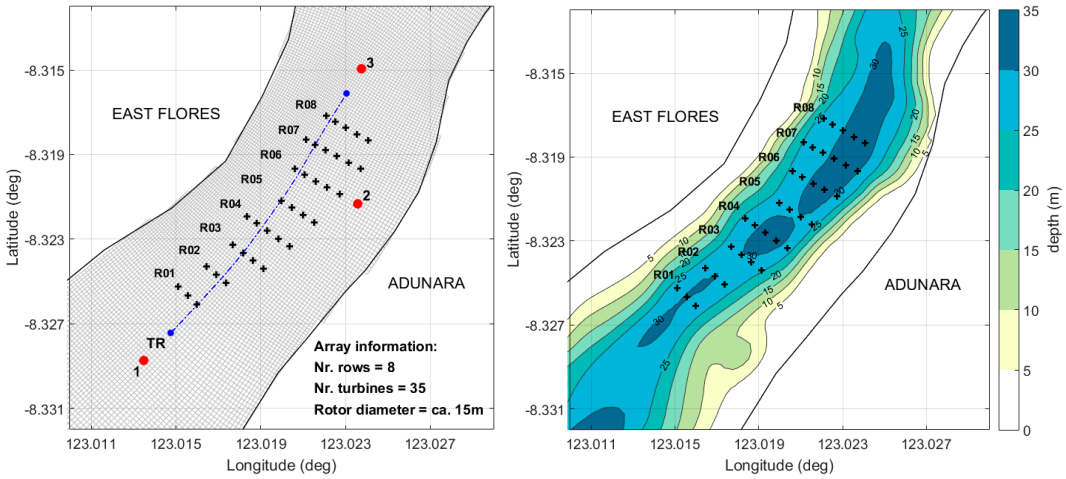

(**a**) (**b**)

Figure 3. Computational grid, observational points 1, 2, and 3 (red marker) and transect TR (blue line) (**a**), bathymetry (**b**), and turbine arrangement due to the proposed layout 4 (**a**, **b**).

Although tidal turbines do not have significant impacts on water levels, they have been predicted to noticeably reduce both upstream and downstream current speeds while increasing them along the side of the array. In the region immediately around the area swept by the turbine, flow also accelerates [29]. In this study, the drag force, induced by the physical structure of turbine blades and supporting poles, is not taken into account. Momentum is assumed to be exchanged only across the rotors and partially dissipated due to the power generation [32]. To capture the impacts of tidal turbines on the surrounding flow field, porous plates set as momentum sinks and covering the faces of single grid cells on several vertical layers have been implemented in the model to represent the tidal current energy extraction [18,32–34]. Considering the power coefficient of the design turbine (C_p = 0.41), the thrust coefficient of the porous plates was chosen as 0.8 (C_t = 0.8) and assumed to be constant for simplicity [32,35]. Thereby, changes in the flow field within and around the arrays, and the wake properties have been determined concerning different array layouts. Turbine arrays deployed with four different layouts were considered. To capture the changes occurring in the flow field in response to increasing array capacities, with each layout, two additional rows of tidal turbines were introduced into the existing arrays. Thus, the proposed layouts consist of 2, 4, 6, and 8 rows of tidal turbines, comprising respectively of a total of 6, 15, 24, and 35 devices. The performances of the

arrays and individual rows/turbines are evaluated for each layout separately, and comparisons among the results of the various layouts are provided.

3. Results

3.1. Flow Field

Figure 4 illustrates the flow field within the farm area in its natural state without the presence of turbines. Figure 4, top panel, shows the time series of simulated depth-averaged current speeds at the observation point 3 (see Figure 3) during July 2014. As can be seen, while peak current speeds reach around 2 m/s during a neap tide, they are much more energetic and exceed 3 m/s during the spring tidal cycle. Figure 4, middle, and Figure 4, bottom illustrate magnitudes and standard deviations of depth and time-averaged current speeds during the flooding stage of a neap (07.07.2014 18:50–08.07.2014 01:10) and a spring (15.07.2014 13:30–15.07.2014 19:50) tidal cycle, respectively. During the flood, the currents in the Strait of Larantuka flow predominantly in the northeast direction, towards the Flores Sea (see Figure 1). It can be noticed that, while depth and time-averaged current speeds are around 1 m/s during the neap tidal cycle, they exceed 2 m/s during the spring tide and show much higher standard deviations. Meanwhile, during both neap and spring tidal cycles, the main channel of the strait, where water depth is above 25 m, remains the most energetic area of the strait, and currents are rather weak closer to the banks (< 0.5 m/s). Thus, in this study, tidal turbine arrays with various capacities have been located at the highly energetic reach of the strait, as shown in Figure 5.

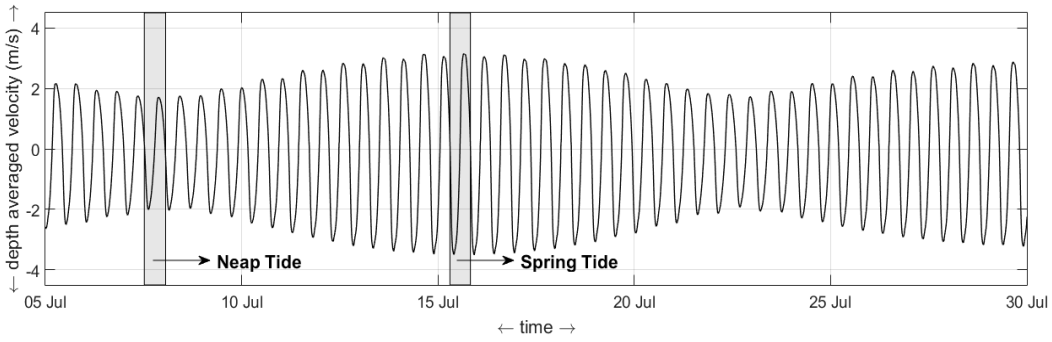

(a)

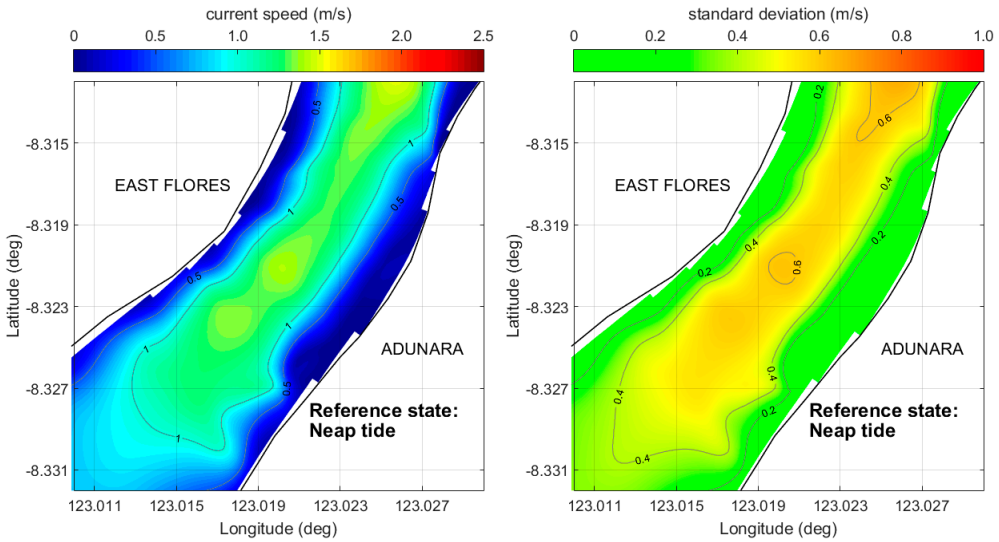

(b)

Figure 4. *Cont.*

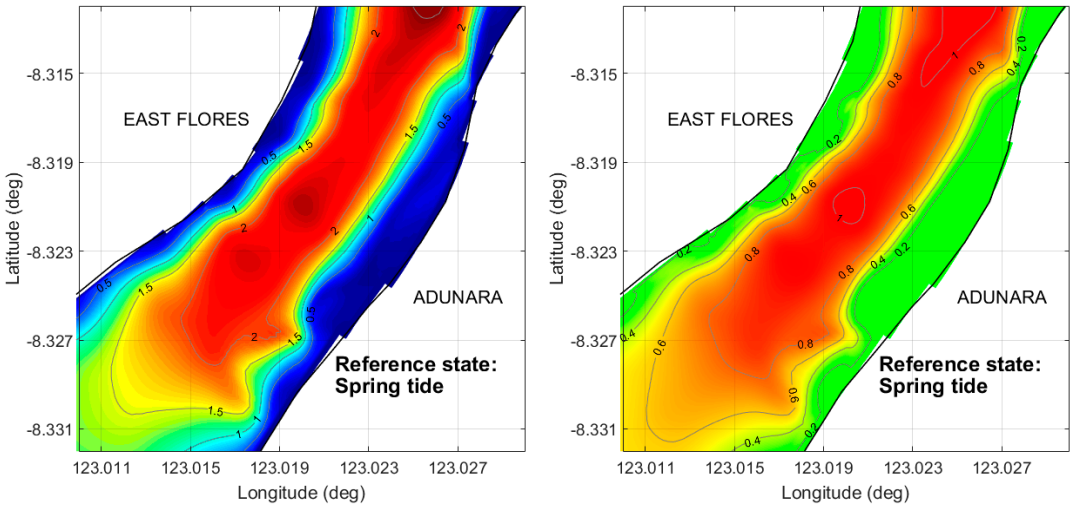

(**c**)

Figure 4. Simulated depth and time-averaged current speeds at the observation point 3 (see Figure 3) during July 2014 (**a**); magnitudes and standard deviations of depth and time-averaged current speeds during the flooding stage of a neap (**b**) and a spring (**c**) tidal cycle (see top panel). Figures illustrate the flow field within the farm area (see Figure 3) in its natural (reference) state.

Figure 5 demonstrates the influence of tidal current energy extraction from the flow field during the spring tide through various turbine arrays. Properties of the tidal turbines considered in the investigations are explained in Section 2. In vertical, the upper 5 m near the free surface was avoided to prevent conflict with recreational activities, such as small boats and swimmers, to minimize turbulence and wave loading effects on the turbines, and to avoid damage from floating materials. At the bottom, the turbines were placed above the low-speed benthic boundary layer, which is approximately 10% of the mean lower low water depth and equals to ca. 3 m within the farm area [11,12,30,36]. It can be seen that, compared to the reference state, the deficit of the current speeds can reach 0.5–0.6 m/s on average during the spring tide due to the chosen layout. In layout 1 (Figure 5, top-left), the change in the flow field is minor (0.1–0.2 m/s deficit). On the other hand, increased numbers of rows and turbines deployed due to the proposed layout 4 (Figure 5, bottom-right) resulted in a deficit of about 0.5–0.6 m/s. This corresponds to decreases in current speeds of about 25%–30% on average.

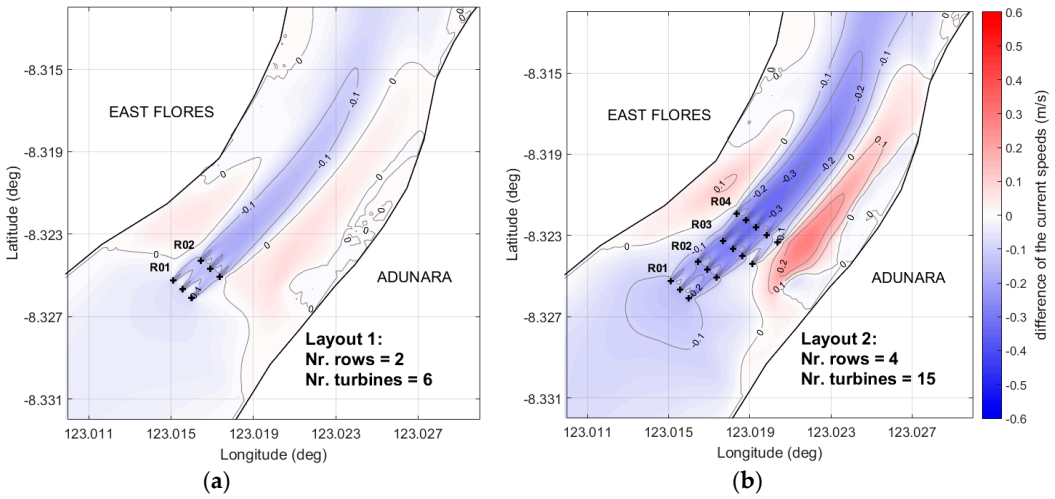

(**a**) (**b**)

Figure 5. *Cont.*

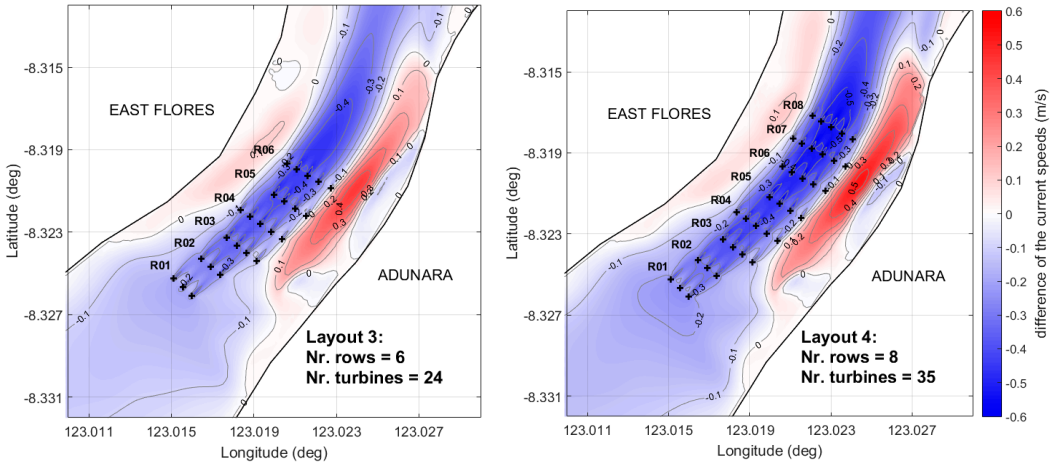

Figure 5. Difference of the depth and time-averaged current speeds (15.07.2014 13:30–15.07.2014 19:50) between the reference state (see Figure 4) and energy extraction scenarios due to proposed arrays with layout 1 (**a**); layout 2 (**b**); layout 3 (**c**); layout 4 (**d**).

Furthermore, as previously pointed out by Ahmadian et al. (2012), besides the decrease in the current speeds, both upstream and downstream of the turbine arrays, stronger current velocities can be observed on the sides, closer to the banks [37]. Especially due to the geometry of the strait and the proximity of turbines to the banks and near-shore shallow waters, bigger impacts resulted closer to Adunara Island. It can be seen that the stronger blockage effects due to the larger number of turbines in layouts 2, 3, and 4 led to increases in the current speeds of up to about 0.5–0.6 m/s on the sides of the arrays. This means that the deployment of tidal turbines with dense layouts in the vicinity of the Adunara Island's shoreline can increase the current speeds in the area by approximately 70%–80%, with respect to the current speeds in the reference state. Meanwhile, during the neap tide, changes observed in the flow field remained insignificant due to the low current speeds. The observed magnitude of both decreases and increases in the current speeds were between 0.1–0.2 m/s even in case of the densest array layouts.

Figure 6, top, depicts the temporal changes in the natural state of the flow field caused by the turbines deployed due to the proposed layout 4 during a half-daily spring tidal cycle consisting of an ebb tide and a flood tide. The time series of current speeds at the observation points 1, 2, and 3 (see Figure 3), reveal the effects of tidal energy extraction on current speeds in adjacent areas (Figure 6, top). Observation points 1 and 3 are located respectively 20 RD upstream and 20 RD downstream of the multi-row array. Although they are on the opposite directions of the turbine arrays, observations from both points demonstrate decreases in currents speeds as compared to the reference state during flood and ebb tides alike. This means that the momentum dissipation caused by the tidal turbine arrays have similar influences on the flow field, both downstream and upstream. On the other hand, time series of the current speeds obtained from the observation point 2 (see Figure 3), close to the Adunara Island, indicate an increase in the current speeds of ca. 0.6 m/s during the flood tide and ca. 0.3 m/s during the ebb tide. As the sediment transport is proportional to the cube of the current speeds, a change in this scale can have a huge impact on the coastline through erosion and degradation [38]. In such situations, measures aimed at protecting the shoreline or alternative sites/layouts for the tidal arrays would be necessary [12,39,40].

Figure 6, bottom, shows the time-averaged current speeds computed along the transect TR (see Figure 3) on three different vertical layers: above, center, and below the turbines. It is visible that there's an overall decrease in current speeds along the centerline, which is aligned with the turbine rotor hub. Compared to the reference state, the decrease in current speeds along the transect can reach 1.1–1.2 m/s. The average velocity deficit caused by the turbines is about 0.5–0.6 m/s, corresponding

to approximately 25%–30% of the current speeds upstream of the devices. Increasing current speeds seemed to occur between laterally aligned turbines, as well as above and below the turbine rotors, indicating stronger current speeds below the free surface and above the benthic layer.

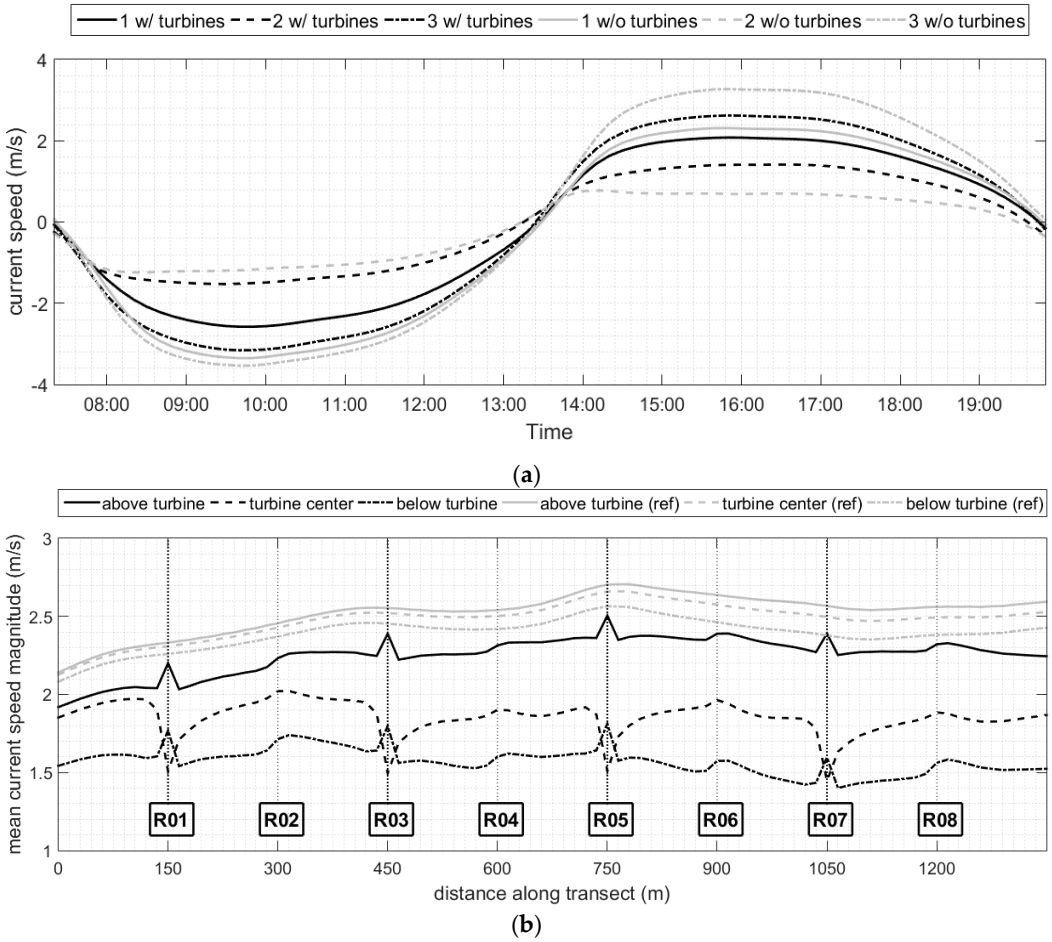

Figure 6. Time-series of depth-averaged currents speeds at the observation points 1, 2, and 3 (see Figure 3) simulated for the spring tidal cycle (see Figure 4a) with (w/) and without (w/o) the turbines, respectively (**a**); time-averaged currents speeds from above, center, and below the turbines over the transect TR (see Figure 3) calculated for the flood tide during the spring tidal cycle (**b**). Plots show the currents speed simulated considering the turbines deployed due to the proposed layout 4 (Figure 5).

3.2. Farm Performance

The method introduced in Orhan et al. (2016) and Orhan and Mayerle (2017) was utilized for the calculation of the extractable electric power of each device. Findings were used to estimate the total power production for each row of turbines (R01–R08) of the proposed layouts (1–4). Current speeds at the hub heights (center flow layer) were used to compute the extractable power of the devices. Rated, cut-in, and cut-out current speeds, as well as the power coefficient of the turbines, were taken into account.

Figure 7 and Table 1 presents the results concerning the spring tidal cycle in detail. As expected, higher levels of energy dissipation occurred in the proposed layout 4 (Figure 7, top). Especially closer to the shoreline of Adunara Island, energy dissipation is higher due to the increased blockage effect along the side banks. On the other hand, the turbine wakes seemed to recover significantly within the 10 RD downstream spacing between the devices, even for the denser layouts 3 and 4. Figure 7, bottom, shows the time series of the total power produced by the tidal arrays. It is found that the arrays with layouts 2, 3, and 4 are unable to reach their rated power productions of 15 MW, 24 MW,

and 35 MW, respectively. Only the array with layout 1 can produce electric power at its rated capacity (6 MW) for around an hour of the six-hour flood phase. Meanwhile, during the neap tidal cycle, due to significantly lower current velocities, the power output of turbine arrays remained negligible. As can be expected, array with the layout 4 provided maximum power output, which was slightly higher than 2 MW.

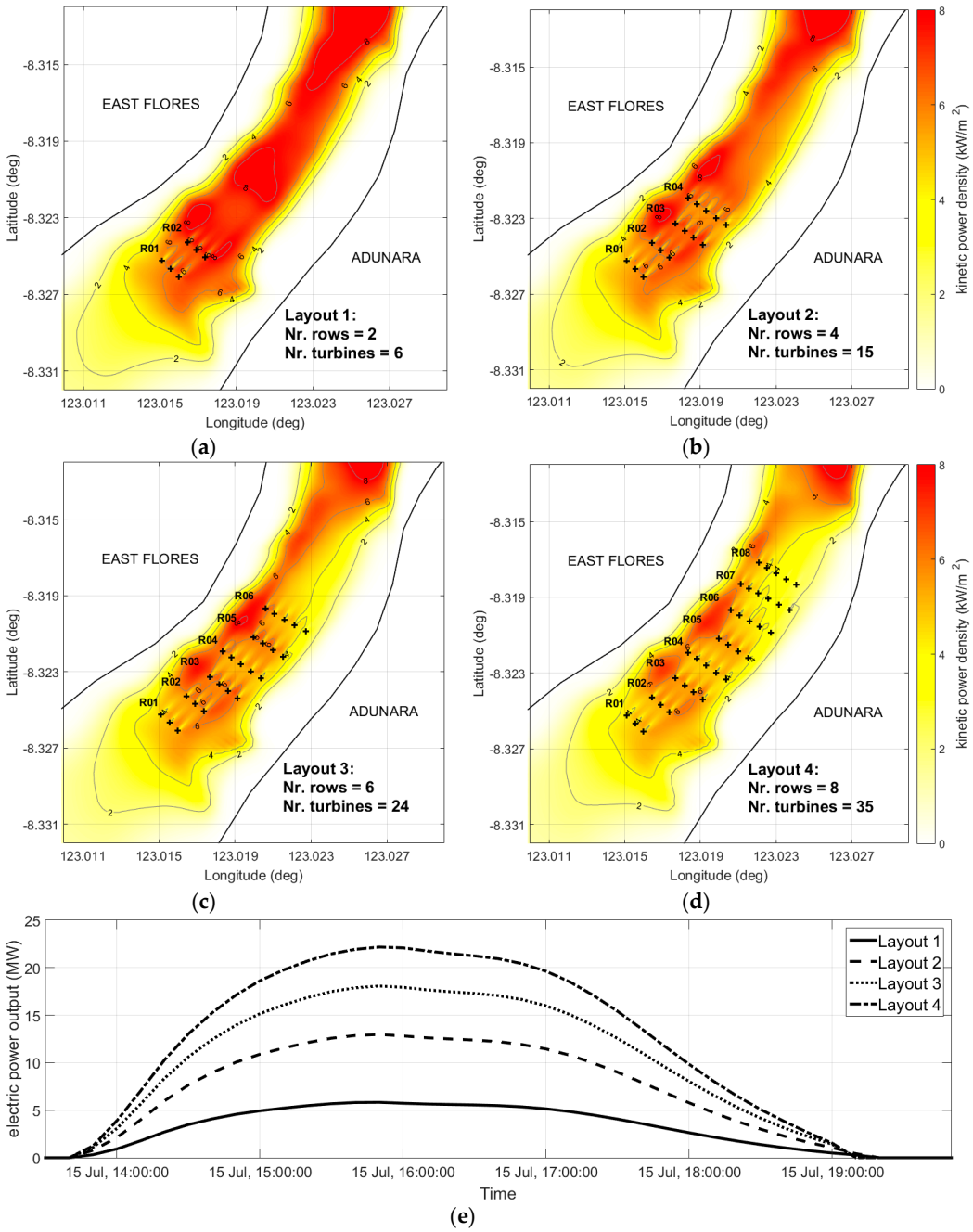

Figure 7. Spatial variation of the average kinetic power densities at the center flow layer during the flood phase of the spring tide (15.07.2014 13:30–15.07.2014 19:50) for arrays with layout 1 (**a**); layout 2 (**b**); layout 3 (**c**); layout 4 (**d**); time series of the total power productions of the arrays during the flood tide (**e**).

Table 1 shows the average electric power produced by each row of all the proposed layouts. It can be noticed that the deployment of additional rows leads to reductions of about 5%–10% in the performance of the turbines upstream. The results are aligned with the findings of Serhadlioglu et

al. (2013) [41]. They pointed out that in case of high blockage ratios, placing arrays in series can reduce arrays efficiencies. Hence to minimize hydro-environmental impacts and maximize energy yield, site-specific factors such as bathymetry, number of turbines, and spatial extents of the designated farm area must be taken into account while choosing the array spacing [42].

Table 1. Time-averaged electric power that can be delivered to the local grid (in megawatt, MW) by tidal turbine rows (R01–08) during the flooding stage of the spring tidal cycle (15.07.2014 13:30–15.07.2014 19:50) considering different array capacities.

Layout	R01 (MW)	R02 (MW)	R03 (MW)	R04 (MW)	R05 (MW)	R06 (MW)	R07 (MW)	R08 (MW)	TOTAL (MW)
1 (R01–02)	1.48	1.60	-	-	-	-	-	-	3.08
2 (R01–04)	1.34	1.43	1.94	2.10	-	-	-	-	6.81
3 (R01–06)	1.23	1.31	1.78	1.91	1.55	1.71	-	-	9.49
4 (R01–08)	1.14	1.21	1.64	1.77	1.44	1.56	1.64	1.25	11.64

The efficiencies of the turbines deployed due to the proposed layouts ($E_{turbine}$) were calculated by comparing the time-averaged operating capacities of the turbines ($P_{average}$) to the rated turbine capacities (P_{rated}), which was assumed 1MW for the devices considered in this study, as follows:

$$E_{turbine} = \frac{P_{average}}{P_{rated}} \quad (1)$$

Figure 8 depicts the estimated efficiencies of the turbines concerning each proposed layout (1–4). Colors indicate the efficiency rate of each turbine. It can be seen that layouts one and two deliver the highest operating efficiency rate of the design turbine. Values up to about 50%–60% are reached. It is also visible that the lowest efficiency rates occur with layout 4. Notice that turbines located behind the array operate with efficiencies around 20%–30%.

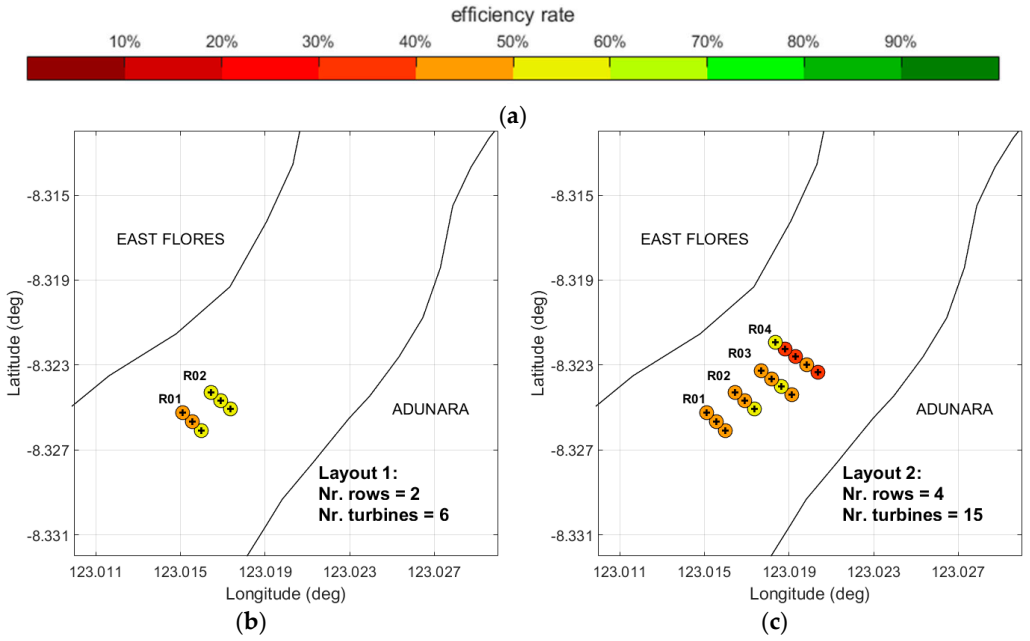

Figure 8. *Cont.*

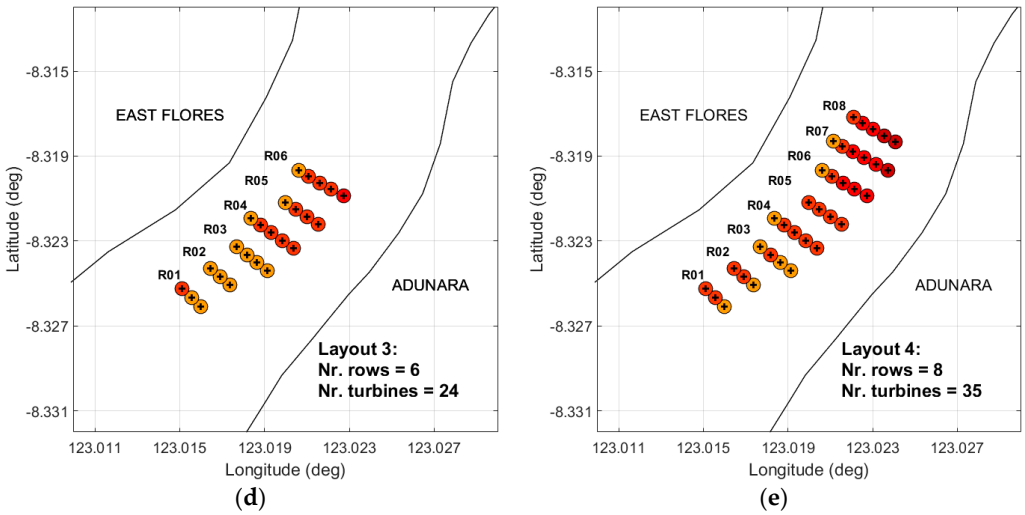

Figure 8. Turbine efficiencies during the flood tide (15.07.2014 13:30–15.07.2014 19:50) in arrays with proposed layout 1 (**b**); layout 2 (**c**); layout 3 (**d**); layout 4 (**e**). The colored markers indicate the efficiency rates of the devices (**a**).

4. Discussion

As it was previously demonstrated by several studies [11,12,14,15], the Strait of Larantuka, located in eastern Indonesia between East Flores and Adunara Island, has a great potential for renewable electricity production from the tidal currents. Hence, the strait is of great commercial interest [15]. However, the potential impacts of the large scale tidal turbine arrays on the flow field of the strait was unknown. It was thought that, in the Strait of Larantuka, large turbine arrays could cause significant changes in the flow field due to the increased geometric blockage effect, which might alleviate the power performances and efficiencies of the tidal turbines. This study aimed at exploring the influence of turbine array capacity and layout on flow conditions, power performances of the turbine arrays, and individual turbine performances. The flow field of the strait was simulated in its natural state, and considering tidal energy extraction scenarios due to four proposed multi-turbine, multi-row arrays. Although tides are the main driving force in the Strait of Larantuka, a baroclinic model was preferred to capture the potential influence of density gradients, as well as the interaction between the Indonesian throughflow and tidal currents. A design turbine, which was assumed capable of harnessing a strong bi-directional flow, was defined based on the properties of state-of-the-art, commercially available tidal turbines. The momentum sink approach was used to account for the influence of tidal energy extraction by the turbines on the flow conditions. For each proposed array, changes in the flow field, wake characteristics, and performances of arrays and turbines were analyzed. Main findings are as follows:

(1) The highly energetic tidal stream currents of the Strait of Larantuka have tremendous potential for renewable electricity production, which might bring huge improvements to the energy portfolio of the region. In their natural states, current speeds exceed 3 m/s in the main channel, while the hydro-kinetic power densities reach 10 kW/m^2 [11,12].

(2) There are huge discrepancies between the impacts and performances of tidal turbines during neap and spring tidal cycles. While the devices have a significant impact on the flow field and provide a considerable power output during the spring tide, during the neap tide, the impact is negligible, and the power output is low.

(3) The decrease in current speeds caused by the tidal energy extraction differs from 0.1 m/s to 0.6 m/s during the spring tide within and around the tidal arrays due to the chosen layout. During the neap tide, deficit in current speeds remained in order of 0.1–0.2 m/s. A drastic increase in currents speeds (80%) was observed along the side banks of Adunara Island during the spring tidal cycle,

mainly because of the proximity of devices to the near-shore shallow waters of the island. Such alterations can have a significant influence over the sediment dynamics within the farm area and in adjacent marine environments. Measures aimed at protecting the shoreline against erosion and degradation or, when necessary, seeking alternative sites/layouts for the tidal arrays is highly recommended [37–40].

(4) During both neap and spring tidal cycles, decreases in current speeds were observed both downstream and upstream of the arrays throughout flood and ebb tides alike. The energy dissipation and the blockage effect of the devices caused an overall change in the flow field and not just downstream of the devices.

(5) Due to the arrangement of the devices in proposed layouts, turbine wakes showed different characteristics as compared to those occurring behind isolated turbines. Current speeds seemed to increase between the laterally aligned turbines as well as above and below the turbine rotors. As indicated in an earlier study [32], increased velocities around the turbine swept area enhance the wake mixing process and therefore accelerates the wake recovery downstream of the tidal turbines.

(6) The arrays with layouts 2, 3, and 4 were unable to reach their rated power productions during the spring tide. Only the turbine array with layout 1 was able to produce electric power at its rated capacity for a significant time. Each time new rows were added downstream of the existing array, there is a 5%–10% reduction in the performances of the rows located upstream. Results confirm the disadvantage of placing turbine fences in series in bounded channels where geometric blockage effect might be an issue [41]. Thus, especially while deploying large scale arrays, it is highly recommended to take site-dependent factors such as bathymetry, number of turbines, and spatial extents of the designated farm area into account while deciding array layouts [30]. In bounded channels, such as the target domain, partial turbine fences closer to the one side of the channel might prove advantageous to reduce geometric blockage effect as well as cabling and shipping costs. It might also be useful to revisit and update the recommendations concerning the spacing between tidal turbines [42].

(7) During the spring tide, the maximum operating efficiency rates of the turbines in the order of 50%–60% resulted in the layouts 1 and 2. The lowest efficiency rates occur with the tidal energy extraction scenario due to layout 4. Turbines located behind the array operate with the efficiencies around 20%–30%. Meanwhile, during the neap tide, turbines performed with efficiencies lower than 10%.

(8) Due to the lack of field data, it was not possible to adequately calibrate and validate the presented model. Tide gauge measurements used for verifying model's capability of simulating water level elevations were limited to a single station. Furthermore, providing a first-hand verification of the model's ability to simulate tidal currents was not possible due to the absence of the current measurements. Nevertheless, despite the sparsity of field data, the detailed hydrodynamic model was able to simulate the flow conditions in the Strait of Larantuka reasonably well. We found that the model output concerning the tidal current speeds in their natural state and deficits in tidal current speeds caused by the turbines are aligned with the measurements provided by the earlier numerical and physical modeling studies [14,31,32,43]. However, enhancing the performance of the model through more comprehensive field surveys might prove highly useful for future investigations. Overcoming such problems related to calibrating and validating models developed for the remote and data-poor regions might be possible through community efforts. Data platforms enabling the efficient sharing of field data between different research groups and open source databases, such as the Global Sea Level Observing System (GLOSS) established by the United Nations Educational, Scientific and Cultural Organization (UNESCO), might prove highly useful for research and development efforts worldwide. Moreover, methods to reduce the uncertainty of the model output in case of scarce field data might be improved as a part of future research efforts [9].

The findings may help us to understand the effects of tidal energy extraction on the hydro-environment, and provide a practical approach to oversee array performances and device efficiencies throughout the development of commercial arrays. Results clearly show that, in bounded channels, increasing array sizes might significantly affect the flow field and undermine performances of the tidal turbines. Therefore, in such domains, it highly recommended to consider site selection for turbine deployment as a continuous process. Thus, optimal locations for the devices can be identified throughout the development of tidal farms, environmental impact can be minimized, and overall performances of the arrays can be maximized. Moreover, since that the results of this study are particularly of interest for bounded channels, further research is recommended concerning the channels with different geometries and physical constraints. Future work concerning the Strait of Larantuka can involve evaluating the relationship between the sediment dynamics and water quality in the strait and tidal turbine arrays. Possible influence of the significant blockage effect caused by tidal turbine arrays deployed in the Strait of Larantuka can be studied on interlinked straits as well as on a regional scale. Moreover, modeling approaches and methods developed within this study can be refined and adopted to resolve the interactions between the tidal turbines and stratified ocean currents, where the tides are negligible.

Author Contributions: Conceptualization, K.O. and R.M.; methodology, K.O.; software, K.O.; validation, K.O. and R.M.; formal analysis, K.O.; investigation, K.O. and R.M.; resources, R.M.; data curation, K.O.; writing—original draft preparation, K.O.; writing—review and editing, R.M.; visualization, K.O.; supervision, R.M.; project administration, R.M.; funding acquisition, R.M. All authors have read and agreed to the published version of the manuscript.

Funding: This study is funded by the German Ministry of Education and Research from March 2012 to February 2016 under grant number 03F0646A.

Acknowledgments: The authors would like to thank the German Ministry of Education and Research (BMBF) for the funding of the project, the Indonesian Agencies "Badan Informasi Geospasial (BIG)" for bathymetric data and "Badan Pengkajian dan Penerapan Teknologi (BPPT)" for supporting the installation and maintenance of the measuring devices in Larantuka, and finally the University of Hamburg (UHH) Institute of Oceanography for providing data access.

Conflicts of Interest: The authors declare no conflict of interest.

References

1. IPCC. Summary for Policymakers. In *Global Warming of 1.5 °C. An IPCC Special Report on the Impacts of Global Warming of 1.5 °C Above Pre-Industrial Levels and Related Global Greenhouse Gas Emission Pathways, in the Context of Strengthening the Global Response to the Threat of Climate Change, Sustainable Development, and Efforts to Eradicate Poverty*; Masson-Delmotte, V., Zhai, P., Pörtner, H.-O., Roberts, D., Skea, J., Shukla, P.R., Pirani, A., Moufouma-Okia, W., Péan, C., Pidcock, R., et al., Eds.; World Meteorological Organization: Geneva, Switzerland, 2018; 32p.
2. Magagna, D.; Uihlein, A. *2014 JRC Ocean Energy Status Report*; Publications Office of the European Union: Luxembourg, 2015.
3. Magagna, D.; Monfardini, R.; Uihlein, A. *JRC Ocean Energy Status Report 2016 Edition*; Publications Office of the European Union: Luxembourg, 2016.
4. Lewis, M.; McNaughton, J.; Márquez-Dominguez, C.; Todeschini, G.; Togneri, M.; Masters, I.; Allmark, M.; Stallard, T.; Neill, S.; Goward-Brown, A.; et al. Power variability of tidal-stream energy and implications for electricity supply. *Energy* **2019**, *183*, 1061–1074. [CrossRef]
5. Ray, R.D.; Egbert, G.D.; Erofeeva, S.Y. A brief overview of tides in the Indonesian Seas. *Oceanography* **2005**, *18*, 74–79. [CrossRef]
6. Gordon, A.L. Oceanography of the Indonesian seas and their throughflow. *Oceanography* **2005**, *18*, 14–27. [CrossRef]
7. Mayer, B.; Damm, P.E.; Pohlmann, T.; Rizal, S. What is driving the ITF? An illumination of the Indonesian throughflow with a numerical nested model system. *Dyn. Atmos. Oceans* **2010**, *50*, 301–312. [CrossRef]
8. Mayer, B.; Damm, P.E. The Makassar Strait throughflow and its jet. *J. Geophys. Res.* **2012**, *117*, C07020. [CrossRef]

9. Goward Brown, A.J.; Lewis, M.; Barton, B.I.; Jeans, G.; Spall, S.A. Investigation of the Modulation of the Tidal Stream Resource by Ocean Currents through a Complex Tidal Channel. *J. Mar. Sci. Eng.* **2019**, *7*, 341. [CrossRef]
10. Orhan, K.; Mayerle, R.; Mayer, B. About the Influence of Density-Induced Flow on Tidal Stream Power Generation in the Sunda Strait, Indonesia. In Proceedings of the 38th IAHR World Congress, Panama City, Panama, 1–6 September 2019.
11. Orhan, K.; Mayerle, R.; Narayanan, R.; Pandoe, W. Investigation of the energy potential from tidal stream currents in Indonesia. *Coast. Eng. Proc.* **2017**, *1*, 10. [CrossRef]
12. Orhan, K.; Mayerle, R. Assessment of the tidal stream power potential and impacts of tidal current turbines in the Strait of Larantuka, Indonesia. *Energy Procedia* **2017**, *125*, 230–239. [CrossRef]
13. Lewis, M.; Neill, S.P.; Robins, P.E.; Hashemi, M.R. Resource assessment for future generations of tidal-stream energy arrays. *Energy* **2015**, *83*, 403–415. [CrossRef]
14. Ajiwibowo, H.; Lodiwa, K.S.; Pratama, M.B.; Wurjanto, A. Field measurement and numerical modeling of tidal current in Larantuka Strait for renewable energy utilization. *Int. J. Geomate* **2017**, *13*, 124–131. [CrossRef]
15. Firdaus, A.M.; Houlsby, G.T.; Adcock, T.A. Tidal Energy Resource in Larantuka Straits, Indonesia. *Proc. Inst. Civ. Eng. Energy* **2019**, 1–38. [CrossRef]
16. Firdaus, A.M.; Houlsby, G.T.; Adcock, T.A. Resource estimates in Lombok Straits, Indonesia. In Proceedings of the Technical Committee of the European Wave and Tidal Energy Conference, Naples, Italy, 1–6 September 2019.
17. Lesser, G.R.; Roelvink, J.V.; Van Kester, J.A.T.M.; Stelling, G.S. Development and validation of a three-dimensional morphological model. *Coast. Eng.* **2004**, *51*, 883–915. [CrossRef]
18. Delft Hydraulics. *Delft3D-FLOW User Manual*; Delft Hydraulics: Delft, The Netherlands, 2006.
19. Olson, C.J.; Becker, J.J.; Sandwell, D.T. A new global bathymetry map at 15 arcsecond resolution for resolving seafloor fabric: SRTM15_PLUS. In Proceedings of the AGU Fall Meeting Abstracts, San Francisco, CA, USA, 15–19 December 2014.
20. Tozer, B.; Sandwell, D.T.; Smith, W.H.F.; Olson, C.; Beale, J.R.; Wessel, P. Global bathymetry and topography at 15 arc sec: SRTM15+. *Earth Space Sci.* **2019**, *6*, 1847–1864. [CrossRef]
21. Brown, A.J.G.; Neill, S.P.; Lewis, M.J. Tidal energy extraction in three-dimensional ocean models. *Renew. Energy* **2017**, *114*, 244–257. [CrossRef]
22. Piano, M.; Robins, P.E.; Davies, A.G.; Neill, S.P. The Influence of Intra-Array Wake Dynamics on Depth-Averaged Kinetic Tidal Turbine Energy Extraction Simulations. *Energies* **2018**, *11*, 2852. [CrossRef]
23. Cornelissen, S.C. Numerical Modelling of Stratified Flows Comparison of the Sigma and z Coordinate Systems. Master's Thesis, Delft University of Technology, Delft, The Netherlands, 2004.
24. Egbert, G.D.; Erofeeva, S.Y. Efficient inverse modeling of barotropic ocean tides. *J. Atmos. Ocean. Technol.* **2002**, *19*, 183–204. [CrossRef]
25. Environmental Modeling Center. *The GFS Atmospheric Model*; Environmental Modeling Center: University Park, MD, USA, 2003.
26. Lane, A. *The Heat Balance of the North Sea*; Proudman Oceanographic Laboratory: Birkenhead, Merseyside, UK, 1989; 46p.
27. Burchard, H.; Baumert, H. On the performance of a mixed-layer model based on the κ-ε turbulence closure. *J. Geophys. Res. Oceans* **1995**, *100*, 8523–8540. [CrossRef]
28. Postma, L.; Stelling, G.S.; Boon, J. 3-dimensional water quality and hydrodynamic modeling in Hong Kong, III. Stratification and water quality. In Proceedings of the 2nd International Symp. on Environmental Hydraulics, Hong Kong, China, 16–18 December 1998.
29. Roberts, A.; Thomas, B.; Sewell, P.; Khan, Z.; Balmain, S.; Gillman, J. Current tidal power technologies and their suitability for applications in coastal and marine areas. *J. Ocean Eng. Mar. Energy* **2016**, *2*, 227–245. [CrossRef]
30. The European Marine Energy Center Ltd. *Assessment of Tidal Energy Resource*; The European Marine Energy Center Ltd.: Stromness, UK, 2009.
31. Chen, Y.; Lin, B.; Lin, J.; Wang, S. Experimental study of wake structure behind a horizontal axis tidal stream turbine. *Appl. Energy* **2017**, *196*, 82–96. [CrossRef]
32. Chen, Y.; Lin, B.; Lin, J. Modelling tidal current energy extraction in large area using a three-dimensional estuary model. *Comput. Geosci.* **2014**, *72*, 76–83. [CrossRef]

33. Defne, Z.; Haas, K.A.; Fritz, H.M. Numerical modeling of tidal currents and the effects of power extraction on estuarine hydrodynamics along the Georgia coast, USA. *Renew. Energy* **2011**, *36*, 3461–3471. [CrossRef]
34. Yang, Z.; Wang, T. Modeling the effects of tidal energy extraction on estuarine hydrodynamics in a stratified estuary. *Estuaries Coasts* **2015**, *38*, 187–202. [CrossRef]
35. Plew, D.R.; Stevens, C.L. Numerical modelling of the effect of turbines on currents in a tidal channel–Tory Channel, New Zealand. *Renew. Energy* **2013**, *57*, 269–282. [CrossRef]
36. Electric Power Research Institute. *Methodology for Estimating Tidal Current Energy Resources and Power Production by Tidal In-Stream Energy Conversion (TISEC) Devices*; Electric Power Research Institute: Palo Alto, CA, USA, 2006.
37. Ahmadian, R.; Falconer, R.A. Assessment of array shape of tidal stream turbines on hydro-environmental impacts and power output. *Renew. Energy* **2012**, *44*, 318–327. [CrossRef]
38. Neill, S.P.; Litt, E.J.; Couch, S.J.; Davies, A.G. The impact of tidal stream turbines on large-scale sediment dynamics. *Renew. Energy* **2009**, *34*, 2803–2812. [CrossRef]
39. Neill, S.P.; Couch, S.J. Impact of Tidal Energy Converter (TEC) array operation on sediment dynamics. In Proceedings of the 9th European Wave and Tidal Energy Conference, Southampton, UK, 5–9 September 2011.
40. Neill, S.P.; Jordan, J.R.; Couch, S.J. Impact of tidal energy converter (TEC) arrays on the dynamics of headland sand banks. *Renew. Energy* **2012**, *37*, 387–397. [CrossRef]
41. Serhadlıoğlu, S.; Adcock, T.A.; Houlsby, G.T.; Draper, S.; Borthwick, A.G. Tidal stream energy resource assessment of the Anglesey Skerries. *Int. J. Mar. Energy* **2013**, *3*, e98–e111. [CrossRef]
42. Fallon, D.; Hartnett, M.; Olbert, A.; Nash, S. The effects of array configuration on the hydro-environmental impacts of tidal turbines. *Renew. Energy* **2014**, *64*, 10–25. [CrossRef]
43. Erwandi Afian, K.; Sasoko, P.; Rina Wijanarko, B.; Marta, E.; Rahuna, D. Vertical Axis Marine Current Turbine Development in Indonesian Hydrodynamic Laboratory-Surabaya for Tidal Power Plant. In Proceedings of the International Conference and Exhibition on Sustainable Energy and Advanced Materials, Solo, Indonesia, 3–4 October 2011.